Journal of Alloys and Compounds 767 (2018) 724–732

Contents lists available at ScienceDirect

Journal of Alloys and Compounds

journal homepage: http://www.elsevier.com/locate/jalcom

NUV light-induced-visible emissions and dopant concentration-dependent optical thermometric behaviors in $Y_2Mo_4O_{15}:2xEr^{3+}$ phosphors

Peng Du, Jae Su Yu*

Department of Electronic Engineering, Kyung Hee University, Yongin-si, Gyeonggi-do 17104, Republic of Korea

ARTICLE INFO

Article history:
Received 16 March 2018
Received in revised form
10 July 2018
Accepted 11 July 2018

Keywords:
Luminescence
Phosphors
Thermometry
Rare-earth

ABSTRACT

We reported the photoluminescence (PL) and optical thermometric properties of Er^{3+}-doped $Y_2Mo_4O_{15}$ phosphors synthesized by a facile sol-gel method. Upon the light excitation at a wavelength of 377 nm, all the compounds emitted visible green emissions with high color purity of 94.8%. A gradual enhancement in PL emission intensity was observed with increasing the Er^{3+} ion concentration in resultant compounds, reaching its optimal value when $x = 0.04$. The concentration quenching mechanism of Er^{3+} ions in the $Y_2Mo_4O_{15}$ host lattice was dominated by the dipole-dipole interaction and the critical distance was estimated to be around 36.7 Å. With the aid of fluorescence intensity ratio technique based on the thermally coupled levels of Er^{3+} ions, the optical thermometric behaviors of the resultant phosphors were studied by analyzing the temperature-dependent PL emission spectra. It was found that the sensor sensitivities of the as-synthesized samples were sensitive to the Er^{3+} ion concentration. The maximum sensor sensitivity of the obtained phosphors reached up to 0.01 K^{-1} at 473 K when the doping concentration was 1 mol%. These observed results reveal that the Er^{3+}-doped $Y_2Mo_4O_{15}$ phosphors have promising applications in noninvasion optical thermometry.

1. Introduction

Temperature is one of the fundamental quantities in many aspects including scientific research, industrial manufacture, medical diagnosis and daily life. As a consequence, its accurate calibration and measurement with high spatial resolution are very necessary. Unfortunately, the commercial contacted thermometers which take the advantage of liquid or metal expansion exhibit some unsatisfactory characteristics, such as long response time, actual temperature change of the objects and limitation of their vivid applications [1,2]. In recent years, the non-contact optical temperature sensor based on the fluorescence intensity ratio (FIR) from two thermally coupled levels of rare-earth ions, which possesses admirable merits of fast response, noninvasion operation mode and high resolution, has received considerable attention [3,4]. To minimize the emission overlap and improve the accuracy, the energy gap of the thermally coupled levels should range from 200 to 2000 cm^{-1} [5,6]. By analyzing the energy level distribution, some rare-earth ions, such as Eu^{3+}, Tm^{3+}, Er^{3+}, Nd^{3+}, Dy^{3+} and Ho^{3+}, were revealed to have a pair of thermally coupled levels and showed a potential applicability for optical thermometry using the FIR technique [7–12]. In comparison, the Er^{3+} ions doped materials are the primary choice to be employed as the luminescent thermometers because of its featured green emissions originating from the $^2H_{11/2}$ and $^4S_{3/2}$ thermally coupled levels with satisfying the energy separation (~770-850 cm^{-1}) [13–15]. It was reported that the $CaSc_2O_4:Er^{3+}/Yb^{3+}$ one-dimensional nanofibers exhibited potential applications in optical temperature sensors with a maximum sensor sensitivity of around 0.004 K^{-1} [16]. Meanwhile, Vetrone et al. also stated that the water soluble $NaYF_4:Er^{3+}/Yb^{3+}$ upconversion nanoparticles were promising nanothermometers for monitoring the temperature distribution of living cells by the FIR technique [17]. Evidently, most of the reports on the optical thermometric properties of Er^{3+} ions-based systems were only focused on the upconverting luminescent materials, whereas the temperature sensing performances of the near-ultraviolet (NUV) light excited Er^{3+}-doped phosphors were scarcely investigated.

As is known, the photoluminescence (PL) properties of rare-earth ions are distinctly dependent on the phonon energy of host materials.

* Corresponding author.
E-mail address: jsyu@khu.ac.kr (J.S. Yu).

https://doi.org/10.1016/j.jallcom.2018.07.143
0925-8388/

Specially, the matrix with low phonon energy is considered as a promising luminescent host material since it can reduce the non-radiative (NR) transition and increase the possibility of radiative transition, leading to high luminescent efficiency [18,19]. Until now, in comparison with other developed inorganic materials, the molydates with outstanding intrinsic optical behaviors (*i.e.*, strong absorption in the ultraviolet region), high stability and facile synthesis have been extensively investigated as the luminescent host materials [20–22]. Li et al. revealed that the Sm^{3+}-doped Lu_2MoO_6 phosphors with bright red emission were suitable for solid-state lighting and temperature sensing [23]. Moreover, the Eu^{3+}-doped $Y_2Mo_4O_{15}$ phosphors were also demonstrated to be a potential candidate for indoor illumination as a red-emitting component [24]. Aside from these, some other impressive results, such as enhanced luminescent performance, strong upconversion emission and multicolor emissions, were also found in rare-earth ions doped molybdates, such as $LiLaMo_2O_8:Eu^{3+}$, $MgMoO_4:Eu^{3+}/Bi^{3+}$, $Y_2Mo_4O_{15}:Ho^{3+}/Yb^{3+}$ and $CsGd(MoO_4)_2:Dy^{3+}/Eu^{3+}$ [25–28]. Nevertheless, to the best of our knowledge, the study on the synthesis, PL performances and optical thermometric behaviors of Er^{3+}-doped $Y_2Mo_4O_{15}$ phosphors has not been reported yet. Therefore, in this work, we selected the $Y_2Mo_4O_{15}$ as the luminescent host material and the citric acid-assisted sol-gel route was employed to prepare the Er^{3+}-doped $Y_2Mo_4O_{15}$ phosphors to explore their feasibility for optical thermometers. The phase structure, microstructure, PL properties and concentration quenching mechanism of the obtained compounds were investigated. Furthermore, by analyzing the temperature-dependent PL emission spectra, the temperature sensing ability of the resultant samples was also studied. Ultimately, the effect of doping concentration on the sensor sensitivities of the synthesized phosphors was systematically analyzed.

2. Experimental process

A simple sol-gel method was employed to prepare $Y_{2(1-x)}Mo_4O_{15}:2xEr^{3+}$ ($Y_2Mo_4O_{15}:2xEr^{3+}$; $x = 0.01$, 0.02, 0.03, 0.04, 0.06 and 0.08) phosphors. High-purity powders of yttrium(III) nitrate hexahydrate ($Y(NO_3)_3\cdot 6H_2O$; 99.8%), ammonium molybdate ($(NH_4)_6Mo_7O_{24}\cdot 4H_2O$; 99.98%), erbium(III) nitrate pentahydrate ($Er(NO_3)_3\cdot 5H_2O$; 99.9%) and critic acid were used as the raw materials. Based on the stoichiometric ratio, (2-2*x*) mmol $Y(NO_3)_3\cdot 6H_2O$, 1 mmol $(NH_4)_6Mo_7O_{24}\cdot 4H_2O$ and 2*x* mmol $Er(NO_3)_3\cdot 5H_2O$ were dissolved in 200 ml of de-ionized water under strong stirring. Subsequently, 12 mmol citric acid was weighted and poured into the above solution. Then, the mixture was sealed with a lid and kept at 80 °C with continuous agitation. After 30 min stirring, the lid was taken away and the mixture was heated at 80 °C to form the wet-gel. Subsequently, the wet-gel was shifted to oven and heated at 120 °C for 12 h to form the xerogel. Finally, the xerogel was annealed at 700 °C for 12 h in air to produce $Y_2Mo_4O_{15}:2xEr^{3+}$ phosphors.

The phase structure and compositions of the final products were examined by using a X-ray diffractometer (Bruker D8 Advance) with Cu Kα radiation and its wavelength was 1.5406 Å. The microstructure and particle size of the prepare samples were analyzed by utilizing a field-emission scanning electron microscope (FE-SEM) (LEO SUPRA 55, Carl Zeiss). The PL excitation (PLE) and PL emission spectra of the as-synthesized compounds were measured by employing a spectrofluorometer (Scinco FluroMate FS-2) and the Xe arc lamp acted as the excitation light source. The temperature ranging from 293 to 473 K was controlled by using a thermocouple (NOVA ST540).

3. Results and discussion

The XRD patterns of Er^{3+}-doped $Y_2Mo_4O_{15}$ phosphors sintered at 700 °C with different doping concentrations are depicted in Fig. 1(a). As presented, all the compounds possessed the same diffraction files and the recorded diffraction peaks were in good agreement with the JCPDS#53-0358 of monoclinic $Y_2Mo_4O_{15}$, revealing that the synthesized samples exhibited pure monoclinic phase and the Er^{3+} ions were totally incorporated into the $Y_2Mo_4O_{15}$ host lattice without inducing any impacts on the crystal structure of the luminescent host material. Besides, it can be seen from the magnificent XRD patterns that the diffraction peaks gradually shifted to the larger angles with elevating the Er^{3+} ion concentration from 1 to 8 mol%, which results in the shrinkage of the host lattice as well as the changed local crystal field surrounding the dopants due to the inconsistent ionic radii between the Y^{3+} (0.96 Å) and Er^{3+} (0.945 Å) ions, as displayed in Fig. 1(b). As we know, to develop a new solid solution, the ionic radius percentage difference (D_r) between the dopants and potential substituted cations can not be over 30 mol%. In term of Y^{3+} and Er^{3+} ions, the D_r value was calculated to be as low as 1.5% using the expression of $D_r = (R_1 - R_2)/R_1 \times 100\%$, where R_1 and R_2 are assigned to the ionic radii of the substituted ions and dopants, respectively [29,30].

To further verify that the Er^{3+} ions were successfully doped into the luminescent host lattice, the Rietveld XRD refinement of the $Y_2Mo_4O_{15}:0.08Er^{3+}$ phosphor was carried out by utilizing the General Structure Analysis System. As shown in Fig. 2(a), the detected and calculated diffraction peaks coincided well with each other, indicating the pure monoclinic phase of the synthesized compounds. Moreover, the reliability factors of the refinement were found to be $R_{wp} = 7.3\%$, $R_p = 5.7\%$ and $\chi^2 = 3.14$, while the refined lattice parameters of the $Y_2Mo_4O_{15}:0.08Er^{3+}$ phosphor were demonstrated to be $a = 6.18676$ Å, $b = 9.58090$ Å, $c = 10.52065$ Å and $V = 661.82$ Å^3 which were smaller than those of the standard $Y_2Mo_4O_{15}$ ($a = 6.1885$ Å, $b = 9.5913$ Å, $c = 10.5299$ Å and $V = 663.31$ Å^3; JCPDS#53-0358) host lattice. These declined cell parameters also revealed the successful substitution of Y^{3+} ions by Er^{3+} ions and formed the $Y_2Mo_4O_{15}:2xEr^{3+}$ compounds.

The Fourier transform infrared (FT-IR) spectrum was used to distinguish the possible surface functional groups of $Y_2Mo_4O_{15}:2xEr^{3+}$ material systems. Fig. 2(b) displays the representative FT-IR spectrum of the $Y_2Mo_4O_{15}:0.08Er^{3+}$ phosphor in the range of 450–4000 cm^{-1}. The weak broad band centered at around 3402 cm^{-1} is assigned to the O-H symmetric stretching vibration [31]. Moreover, the bands at approximately 957 and 845 cm^{-1} are related to the antisymmetric stretching vibrations of Mo-O bond, whereas the absorption at 766 cm^{-1} corresponds to the vibrational mode of Mo-O-Mo bond [32].

To examine the elemental components of the resultant samples, the XPS spectra of the $Y_2Mo_4O_{15}:0.08Er^{3+}$ phosphor were taken

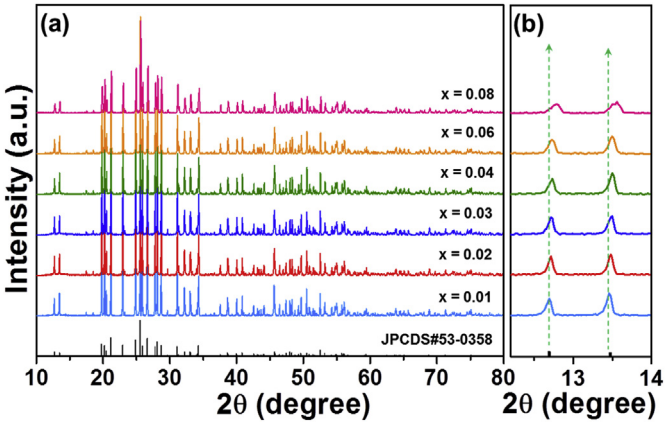

Fig. 1. (a) XRD patterns of $Y_2Mo_4O_{15}:2xEr^{3+}$ phosphors with different doping concentrations. (b) Magnified XRD patterns in the range of 12.2–14°.